Exploring the effects of Delta Baryons in magnetars

Kauan Dalfovo Marquez

marquezkauan@gmail.com

UNIVERSIDADE FEDERAL
DE SANTA CATARINA

with the collaboration of
D. P. Menezes, V. Dexheimer, D. Chatterjee, M. R. Pelicer and B. C. T. Backes

25/10/2022

- DEXHEIMER, V.; MARQUEZ, K. D.; MENEZES, D. P. Delta baryons in neutron-star matter under strong magnetic fields. EUROPEAN PHYSICAL JOURNAL A 57 216, 2021. [arXiv:2103.09855]
- BACKES, B. C. T.; MARQUEZ, K. D.; MENEZES, D. P. Effects of strong magnetic fields on the hadron-quark deconfinement transition. EUROPEAN PHYSICAL JOURNAL A 57 229, 2021. [arXiv:2103.14733]
- MARQUEZ, K. D.; PELICER, M. R.; GHOSH, S.; PETERSON, J.; CHATTERJEE, D.; DEXHEIMER, V.; MENEZES, D. P. Exploring the effects of Delta Baryons in magnetars. PHYSICAL REVIEW C 106 035801, 2022. [arXiv:2205.09827]

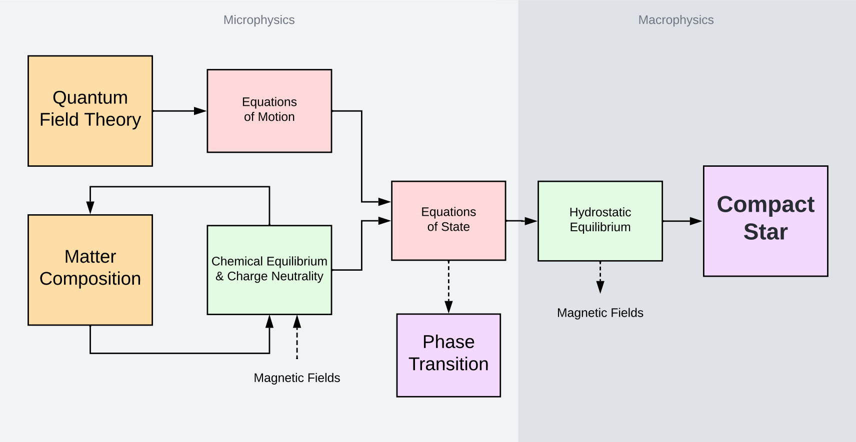
Microphysics
Macrophysics
Quantum Field Theory
Equations of Motion
Matter Composition
Chemical Equilibrium & Charge Neutrality
Magnetic Fields
Equations of State
Phase Transition
Hydrostatic Equilibrium
Magnetic Fields
Compact Star

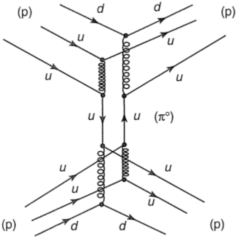

$$
\begin{aligned}
L = \sum_b \Big[\; {}_b \quad i@ \quad g_{!\,b}\,! \quad g\;{}_b \quad \frac{g\;{}_b}{2}\sim \quad \sim \qquad M \Big]_b \\
+ \frac{1}{2}(@ \quad @ \qquad m^2 \quad {}^2) \quad \frac{1}{3} \; {}^3 \quad \frac{{}^2}{4} \; {}^4 \\
\frac{1}{4} \qquad + \frac{1}{2}m_!^2 \, ! \quad ! \qquad \frac{1}{4} \qquad + \frac{1}{2}m^2 \\
\frac{1}{4}\bar{R} \qquad \bar{R} \quad + \frac{1}{2}m^2\sim \quad \sim \quad + g_! \quad ! \quad ! \; \sim \quad \sim \; ; \qquad (1)
\end{aligned}
$$

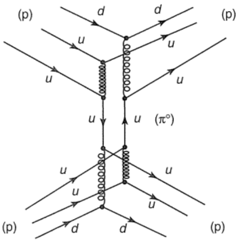

$$\mathcal{L} = \sum_b \left[i\partial \quad g_{\omega b}\,\omega \quad g_{\ b} \quad \frac{g_{\ b}}{2}\vec{\ }\ \vec{\ } \quad M \right]_b$$
$$+ \frac{1}{2}(\partial \quad \partial \quad m^2\ ^2) \quad \frac{1}{3}\ ^3 \quad \frac{2}{4}\ ^4$$
$$\frac{1}{4} \quad + \frac{1}{2}m_\omega^2\,\omega\ \omega \quad \frac{1}{4} \quad + \frac{1}{2}m^2$$
$$\frac{1}{4}\vec{R} \quad \vec{R} \quad + \frac{1}{2}m^2\vec{\ } \quad \vec{\ } \quad + g_\omega \quad \omega \quad \omega\ \vec{\ } \quad \vec{\ }\ ; \qquad (1)$$

Model	n_0	B/A	K	S	L	M/m
GM1	0.153	16.33	300.5	32.5	94	0.70
L3ω	0.156	16.20	256	31.2	74	0.69
DDME2	0.152	16.14	251	32.3	51	0.57
Constr.	0.148−0.170	15.8−16.5	220−260	28.6−34.4	36.0−86.8	0.6−0.8

Table: symmetric nuclear matter properties at saturation density for the models employed in this work.

$${}_{b} = {}_{n} \quad q_{b} \quad {}_{e} \tag{2}$$

$$\sum_{i=b;l} q_i n_i = 0 \tag{3}$$

$$_b = \quad _n \quad q_b \quad _e \tag{2}$$

$$\sum_{i=b;l} q_i n_i = 0 \tag{3}$$

$$'' = \sum_b \frac{1}{\ ^2} \int_0^{p_{F_b}} dp\, p^2 \sqrt{p^2 + M_b^2} + \frac{1}{2} m^2 \ \ _0^2 + \frac{\ ^1}{3} \ \ _0^3 + \frac{\ ^2}{4} \ \ _0^4$$

$$\frac{1}{2} m_!^2 \, !_0^2 \quad \frac{1}{2} m^2 \ \ _0^2 \quad \frac{1}{2} m^2 \ \ _0^2 \quad g_! \quad !_0^2 \ \ _0^2 + ''_{\text{leptons}}; \tag{4}$$

$$P = \quad '' + \sum_b \quad _b n_b \tag{5}$$

$$_b = \quad _n \quad q_b \quad _e \tag{2}$$

$$\sum_{i=b;l} q_i n_i = 0 \tag{3}$$

$$'' = \sum_b \frac{1}{\quad ^2} \int_0^{p_{F_b}} dp\, p^2 \sqrt{p^2 + M_b^2} + \frac{1}{2} m^2 \quad _0^2 + \frac{1}{3} \quad _0^3 + \frac{\quad ^2}{4} \quad _0^4$$

$$\frac{1}{2} m_!^2 \, !_0^2 \quad \frac{1}{2} m^2 \quad _0^2 \quad \frac{1}{2} m^2 \quad _0^2 \quad g_! \quad !_0^2 \quad _0^2 + ''_{\text{leptons}}; \tag{4}$$

$$P = \quad '' + \sum_b \quad _b n_b \tag{5}$$

$$\frac{dP}{dr} = \quad \frac{[''(r) + P(r)] \quad m(r) + 4 \quad r^3 P(r)}{r\,[r \quad 2m(r)]}; \tag{6}$$

$$m(r) = \int_0^r dr' 4 \quad r'^2 \, ''(r') : \tag{7}$$

	M_b (MeV)	$q_b(e)$	$I_{3\,b}$	S_b	$_b=\ _N$	$_b=\ _N$
p	939	+1	+1=2	1/2	2:79	1:79
n	939	0	1=2	1/2	1:91	1:91
	1116	0	0	1/2	0:61	0:61
+	1193	+1	+1	1/2	2:46	1:67
0	1193	0	0	1/2	1:61	1:61
	1193	1	1	1/2	1:16	0:37
0	1315	0	+1=2	1/2	1:25	1:25
	1315	1	1=2	1/2	0:65	0:06
+ +	1232	+2	+3=2	3/2	4:99	3:47
+	1232	+1	+1=2	3/2	2:49	1:73
0	1232	0	1=2	3/2	0:06	0:06
	1232	1	3=2	3/2	2:45	1:69

$$g_{ib} = x_{ib} g_i \tag{8}$$

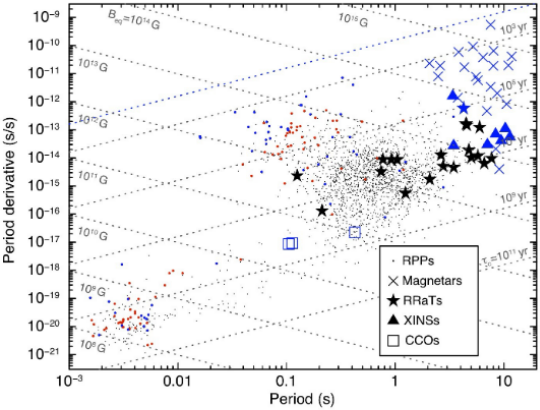

Figure 2 The P–$\dot{P}$ diagram illustrating the placement of the different isolated neutron star classes. The blue dots mark pulsars detected both in the radio and X-ray bands, the red ones those observed only at X-ray energies. The lines of constant age and magnetic field are also shown (courtesy R.P. Mignani).

$$\int d^3k \rightarrow \frac{|q|B}{(2\pi)^2} \sum_{\nu} \int dk_z; \qquad \text{where} \qquad \nu = n + \frac{1}{2} - \frac{s}{2}\frac{q_b}{|q_b|} \tag{9}$$

$$\nu_{\max b}(s) = \left\lfloor \frac{\left(E_{F\,b} + s\,\kappa_b B\right)^2 - M_b^{*2}}{2|q_b|B} \right\rfloor \tag{10}$$

$$\int d^3k \to \frac{|q|B}{(2\pi)^2}\sum_{\nu}\int dk_z; \qquad \text{where} \qquad \nu = n + \frac{1}{2} - \frac{s}{2}\frac{q_b}{|q_b|} \tag{9}$$

$$\nu_{\max b}(s) = \left\lfloor \frac{\left(E_{Fb} + s\mu_b B\right)^2 - M_b^{2}}{2|q_b|B} \right\rfloor \tag{10}$$

$q_b = 0$:

$$k_{F,b}^2(s) = E_{Fb}^{2} - \left(M_b - s\mu_b B\right)^2 \tag{11}$$

$$n_b = \frac{1}{2\pi^2}\sum_s \left\{ \frac{k_{Fb}^3(s)}{3} - \frac{s\mu_b B}{2}\left[\left(M_b - s\mu_b B\right) k_{Fb}(s) + E_{Fb}^{2}\left(\arcsin\left(\frac{M_b - s\mu_b B}{E_{Fb}}\right) - \frac{\pi}{2} \right) \right] \right\} \tag{12}$$

$$n_{sb} = \frac{M_b}{4\pi^2}\sum_s \left[E_{Fb}k_{Fb}(s) - \left(M_b - s\mu_b B\right)^2 \ln\left|\frac{k_{Fb}(s) + E_{Fb}}{M_b - s\mu_b B}\right| \right] \tag{13}$$

$q_b \neq 0$:

$$k_{F,b}^2(\nu, s) = E_{Fb}^{2} - \left(\sqrt{M_b^{2} + 2\nu|q_b|B} - s\mu_b B\right)^2 \tag{14}$$

$$n_b = \frac{|q_b|B}{2\pi^2}\sum_{\nu,s} k_{Fb}(\nu, s) \tag{15}$$

$$n_{sb} = \frac{|q_b|BM_b}{2\pi^2}\sum_{s,\nu} \frac{\sqrt{M_b^{2} + 2\nu|q_b|B} - s\mu_b B}{\sqrt{M_b^{2} + 2\nu|q_b|B}} \ln\left|\frac{k_{Fb}(\nu, s) + E_{Fb}}{\sqrt{M_b^{2} + 2\nu|q_b|B} - s\mu_b B}\right| \tag{16}$$

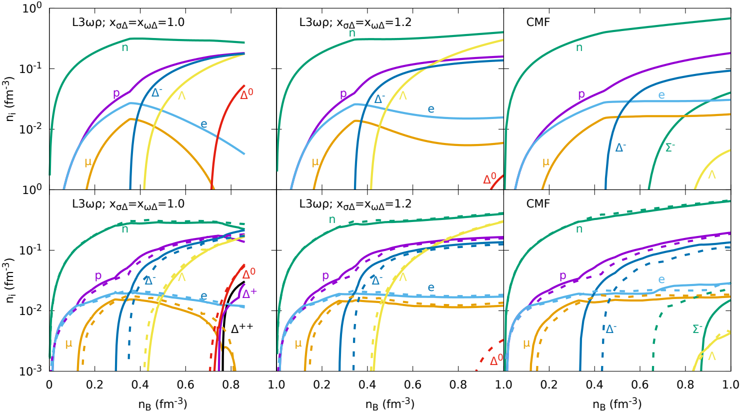

Figure: Particle composition of neutron-star matter with s, with $B = 0$ (top panels) and magnetic field $B = 3 \quad 10^{18}$ G (bottom panels), when considering (solid lines) or disregarding (dashed lines) the effects of the AMMs.

$$Y_{\rm spin} = \frac{\sum_{b,s} s n_b(s)}{\sum_{b,s} n_b(s)} \, ; \tag{17}$$

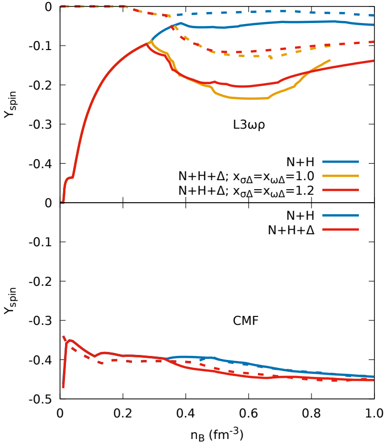

Figure: Spin polarization fraction as a function of baryon number density for neutron-star matter with magnetic field $B = 3 \times 10^{18}$ G, when considering (solid lines) or disregarding (dashed lines) the effects of the AMMs.

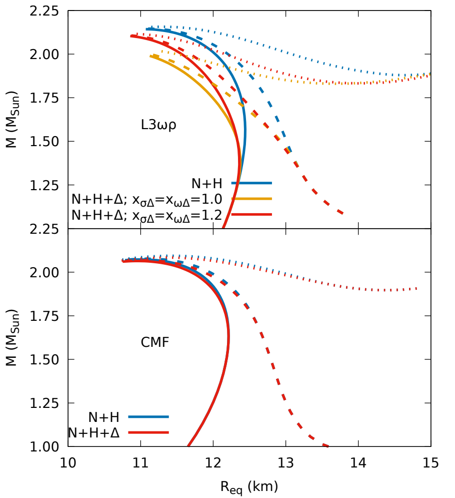

Figure: Stellar mass as a function of equatorial radius for different compositions and interaction strengths, for central magnetic fields $B = 0$ (solid lines), $B = 5 \quad 10^{17}$ G (dashed lines), and $B = 10^{18}$ G (dotted lines).

B (G)	n_c (fm ^{3})		$''_c$ (MeV=fm^3)	
	N+H	N+H+	N+H	N+H+
0	0.672	0.618 (0.614)	742	658 (657)
5 10^{17}	0.701	0.659 (0.653)	783	712 (708)
1 10^{18}	0.747	0.714 (0.707)	850	786 (783)
0	0.629	0.625	678	672
5 10^{17}	0.680	0.677	747	741
1 10^{18}	0.749	0.746	843	837

Table: Central baryon (n_c) and energy ($''_c$) densities as a function of magnetic field strength for neutron stars of radius 12 km with L3 ! model for $x \quad = x_{!} \quad = 1{:}0(1{:}2)$ in the top panel and CMF model in the bottom panel.

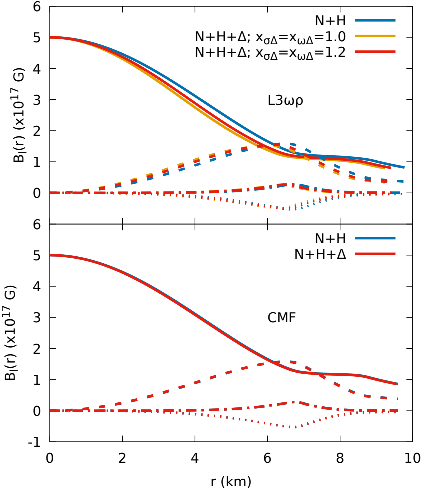

Figure: Magnetic field distribution inside a neutron star of mass $1{:}8M$ and central magnetic field of $B = 5 \quad 10^{17}$ G. Solid, dashed, dashed-dotted and dotted are, respectively, the first four even multipoles of the magnetic field norm ($l = 0; 2; 4; 6$).

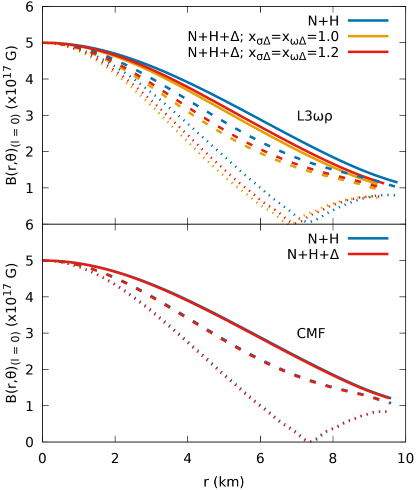

Figure: Magnetic field distribution inside a neutron star of mass $1{:}8M$ and central magnetic field of $B = 5 \quad 10^{17}$ G. Solid, dashed and dotted are the dominant monopolar ($l = 0$) term at the polar ($= 0$), intermediate ($= \quad =4$) and equatorial ($= \quad =2$) orientations.

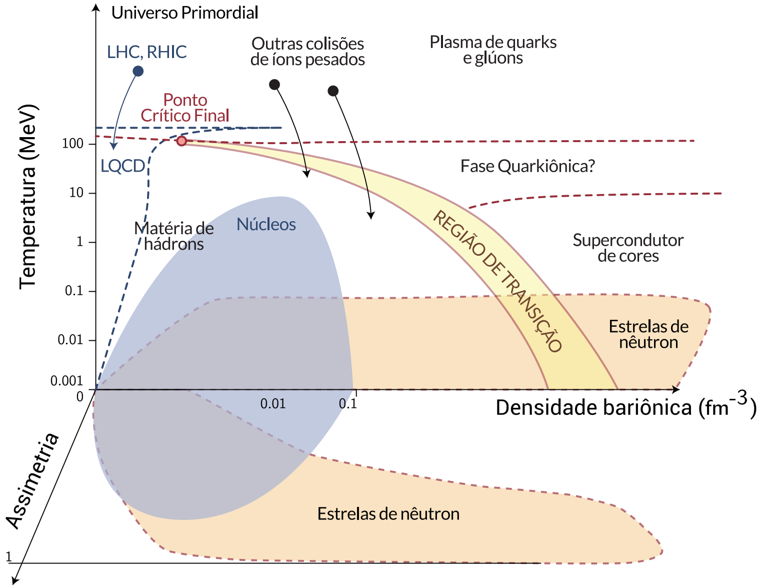
Universo Primordial
LHC, RHIC
Outras colisões de íons pesados
Plasma de quarks e glúons
Ponto Crítico Final
LQCD
Fase Quarkiônica?
REGIÃO DE TRANSIÇÃO
Matéria de hádrons
Núcleos
Supercondutor de cores
Estrelas de nêutron
Temperatura (MeV)
100
10
1
0.1
0.01
0.001
0
0.01
0.1
Densidade bariônica (fm^{-3})
Assimetria
1
Estrelas de nêutron

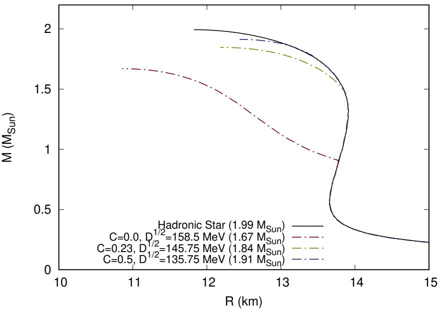

Figure: Mass-radius diagram for hybrid EoS with chemical equilibrium in both phases, showing results without magnetic field effects.

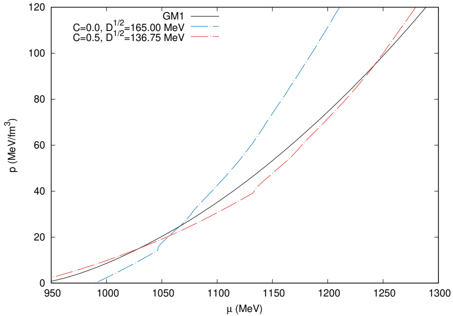

Figure: Example of equations of state of parameter choices that allow the hadron-quark phase transition to occur at $B = 3 \quad 10^{18}$ G.

$$m_i = m_{i0} + \frac{D}{n_b^{1=3}} + Cn_b^{1=3} = m_{i0} + m_I; \tag{18}$$

	B = 0	B = 3 10^{18} G	B-W
p $C = 0$ $\overline{D} = 155$ MeV	no crossing	no crossing	yes
p $C = 0$ $\overline{D} = 158.5$ MeV	$_0 = 960$ $p_0 = 1.55$	$_0 = 958$ $p_0 = 1.80$	yes
p $C = 0$ $\overline{D} = 165$ MeV	$_0 = 1062$ $p_0 = 21.98$	$_0 = 1066$ $p_0 = 24.70$	no
p $C = 0.23$ $\overline{D} = 155$ MeV	$_0 = 1130$ $p_0 = 43.62$	$_0 = 1145$ $p_0 = 51.32$	no
p $C = 0.365$ $\overline{D} = 142$ MeV	$_0 = 1105$ $p_0 = 34.98$	$_0 = 1109$ $p_0 = 38.30$	yes
p $C = 0.5$ $\overline{D} = 135.75$ MeV	$_0 = 1202$ $p_0 = 72.66$	$_0 = 1242$ $p_0 = 94.93$	yes
p $C = 0.68$ $\overline{D} = 130$ MeV	$_0 = 1440$ $p_0 = 215.50$	$_0 = 1475$ $p_0 = 247.53$	yes

Table: Values for $_0$ (in MeV) and p_0 (in MeV/fm^3) for which the conditions of phase coexistence are satisfied at $T = 0$. The latter column specifies whether or not the Bodmer-Witten conjecture is satisfied.

- The understanding of the meson-delta coupling parameters can be refined by symmetry group considerations, as it is made for the hyperon coupling schemes.
- The magnetic field effects on -admixed matter can be more robustly understood by having the complete solution of the spin-3/2 Rarita-Schwinger equation under a magnetic field.

- The understanding of the meson-delta coupling parameters can be refined by symmetry group considerations, as it is made for the hyperon coupling schemes.
- The magnetic field effects on -admixed matter can be more robustly understood by having the complete solution of the spin-3/2 Rarita-Schwinger equation under a magnetic field.

Muito Obrigado!

Kauan Dalfovo Marquez
marquezkauan@gmail.com

PPGFSC

Exploring the effects of Delta Baryons in magnetars

Kauan Dalfovo Marquez

marquezkauan@gmail.com

UNIVERSIDADE FEDERAL
DE SANTA CATARINA

with the collaboration of
D. P. Menezes, V. Dexheimer, D. Chatterjee, M. R. Pelicer and B. C. T. Backes

25/10/2022